

## PDF hosted at the Radboud Repository of the Radboud University Nijmegen

The following full text is a publisher's version.

For additional information about this publication click this link.

<http://hdl.handle.net/2066/173571>

Please be advised that this information was generated on 2020-10-23 and may be subject to change.

## The influence of the atmospheric refractive index on radio $X_{\max}$ measurements of air showers

Arthur Corstanje<sup>1,\*</sup>, Stijn Buitink<sup>2</sup>, Antonio Bonardi<sup>1</sup>, Heino Falcke<sup>1,3,4</sup>, Jörg R. Hörandel<sup>1,4</sup>, Pragati Mitra<sup>2</sup>, Katie Mulrey<sup>2</sup>, Anna Nelles<sup>5</sup>, Jörg Paul Rachen<sup>1</sup>, Laura Rossetto<sup>1</sup>, Pim Schellart<sup>1</sup>, Olaf Scholten<sup>6,7</sup>, Satyendra Thoudam<sup>1</sup>, Gia Trinh<sup>6,7</sup>, Sander ter Veen<sup>3</sup>, and Tobias Winchen<sup>2</sup>

<sup>1</sup>Department of Astrophysics/IMAPP, Radboud University, P.O. Box 9010, 6500 GL Nijmegen (the Netherlands)

<sup>2</sup>Vrije Universiteit Brussel, Pleinlaan 2, 1050 Brussels (Belgium)

<sup>3</sup>Astron, Oude Hoogeveensedijk 4, 7991 PD Dwingeloo (The Netherlands)

<sup>4</sup>Nikhef, Science Park 105, 1098 XG Amsterdam (The Netherlands)

<sup>5</sup>University of California Irvine, Irvine, CA 92697, (USA)

<sup>6</sup>KVI-CART, Zernikelaan 25, 9747 AA Groningen (The Netherlands)

<sup>7</sup>University of Groningen, Zernikelaan 25, 9747 AA Groningen (The Netherlands)

**Abstract.** The refractive index of the atmosphere, which is  $n \approx 1.0003$  at sea level, varies with altitude and with local temperature, pressure and humidity. When performing radio measurements of air showers, natural variations in  $n$  will change the radio lateral intensity distribution, by changing the Cherenkov angle. Using CoREAS simulations, we have evaluated the systematic error on measurements of the shower maximum  $X_{\max}$  due to variations in  $n$ . It was found that a 10 % increase in refractivity ( $n - 1$ ) leads to an underestimation of  $X_{\max}$  between 8 and 22 g/cm<sup>2</sup> for proton-induced showers at zenith angles from 15 to 45 degrees, respectively.

### 1 Introduction

Measurements of the radio emission from air showers, together with microscopic simulations, form a useful method to infer their defining physical quantities, such as primary energy [1] and the depth of shower maximum  $X_{\max}$  [2]. The latter is sensitive to the composition of the primary particles.

Using the densely instrumented inner region of the LOFAR radio telescope [3] has allowed to sample the radio lateral intensity distribution ('footprint') in close detail, and to infer  $X_{\max}$  to a precision of 20 g/cm<sup>2</sup> [2]. This precision is comparable with more common fluorescence measurements (see e.g. [4]), and good for detailed composition studies [5]. In a central ring of 320 m diameter, one can use nearly 300 dual-polarized antennas, operating in the 30 – 80 MHz band. Outside this ring, 18 more stations of 96 antennas are spread over an area of 6 km<sup>2</sup>. LOFAR has measured the radio signals from air showers since 2011 [6]. For the  $X_{\max}$  measurement, the measured radio footprints are compared to simulated footprints, using the CoREAS simulation package [7] for the radio emission, and CORSIKA [8] for the particles in the air showers.

---

\*e-mail: a.corstanje@astro.ru.nl

In CORSIKA and CoREAS, the US Standard atmosphere [9] is taken by default as the model atmosphere. It features a constant temperature lapse rate of  $L = 6.5 \text{ K/km}$ , zero humidity, and a pressure altitude profile given by

$$T(h) = T_0 - Lh, \quad (1)$$

$$p(h) = p_0 \left( \frac{T(h)}{T_0} \right)^{\frac{gM}{LR}}. \quad (2)$$

Standard values are  $p_0 = 1013.25 \text{ hPa}$ ,  $T_0 = 288.15 \text{ K}$ ,  $g = 9.80665 \text{ m/s}^2$ ,  $R = 8.31447 \text{ J/(mol K)}$  and  $M = 0.0289644 \text{ kg/mol}$ . For more realistic circumstances, humidity can be added as a non-zero partial pressure of water vapour  $p_w$ . The refractivity  $N = 10^6 (n - 1)$  is given by [10]

$$N = 77.6890 \frac{p_d}{T} + 71.2952 \frac{p_w}{T} + 375463 \frac{p_w}{T^2}, \quad (3)$$

with  $p_w$  and dry-air pressure  $p_d$  in hPa, and  $T$  in K.

In CoREAS, a default refractivity is taken as  $N = 292$  at sea level. Using the above formulas, we obtain refractivity values at altitudes 3 and 5 km as a function of sea-level temperature, Fig. (1) and Fig. (2). Shown is the relative correction in % to the CoREAS default. It is seen that at lower altitudes,  $N$  is generally overestimated by about 2%, with a large spread with humidity at higher temperatures. At higher altitudes, relevant for slanted air showers,  $N$  is overestimated by about 4%. Below we evaluate the effect of a 10% change in refractivity on measurements of  $X_{\max}$ ; a more accurate treatment of the simulations, by including local atmospheric data from the GDAS database [11] is under investigation.

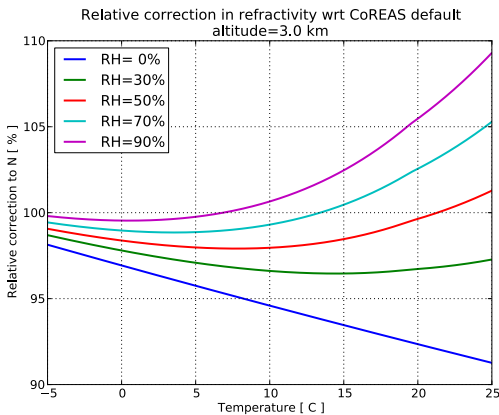


**Figure 1.** Correction to default refractivity, versus sea-level temperature, at 3 km altitude and relative humidity  $RH$ .

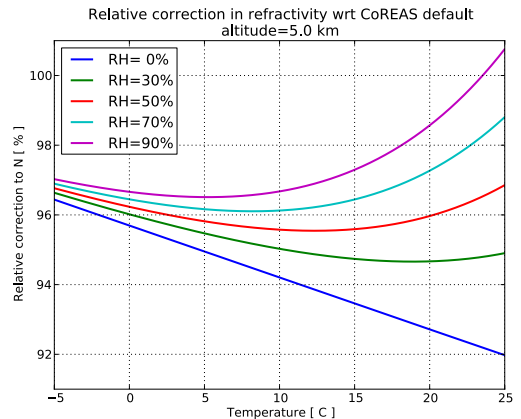


**Figure 2.** Idem at 5 km altitude.

## 2 Method

Using CoREAS simulations, we have determined the systematic offset in  $X_{\max}$  measurements for a 10% increase in refractivity. For proton primary particles coming in at four different zenith angles,

we have created 50 simulated showers at a default refractivity of  $N = 292$  at sea level, and 50 showers at a 10% higher refractivity. The refractivity at higher altitudes is proportional to air density for dry air, and is taken as such in the simulations, which currently assume dry air.

The two ensembles of showers are compared, by taking one shower from the higher-refractivity ensemble, and fitting the lateral intensity distribution by all 50 from the normal- $N$  ensemble. A mean squared error is used as a fit quality measure. This method is similar to [2], where we compare two simulated ensembles, instead of simulation versus data. As the simulated  $X_{\max}$  is known for all showers, the optimum in the fit quality (fitted  $X_{\max}$ ) is compared to the true  $X_{\max}$ . Due to natural shower-to-shower fluctuations, scatter arises in the fit quality plots; an example is shown in Fig. (4). To lowest order, the fit quality is a quadratic function of  $X_{\max}$  near its optimum. Therefore, we fit the points with a parabola. A weighting factor of  $1/y^2$  is introduced to put more emphasis on well-fitting showers, increasing precision of the  $X_{\max}$ -fit by about 20%.

Averaging fitted minus true  $X_{\max}$  over the 50 showers yields the systematic offset in  $X_{\max}$ . We compare the simulation results with a simplistic model, assuming the size of the radio footprint scales with the Cherenkov angle at the  $X_{\max}$  altitude. The altitude-dependent Cherenkov angle  $\alpha$  is given by

$$\cos \alpha = \frac{1}{\beta n(h)}. \quad (4)$$

The model is depicted schematically in Fig. (3). It is expected to hold qualitatively for higher frequencies, above 100 MHz, as for these frequencies, a clear Cherenkov ring is observed both in simulations and in LOFAR data [12].

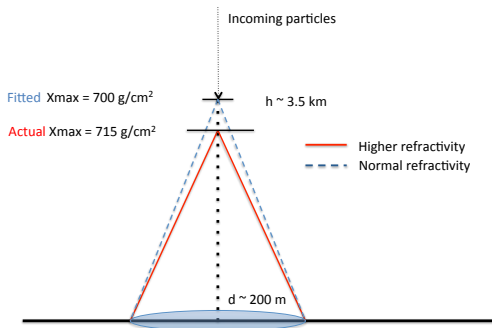


**Figure 3.** Cherenkov model.

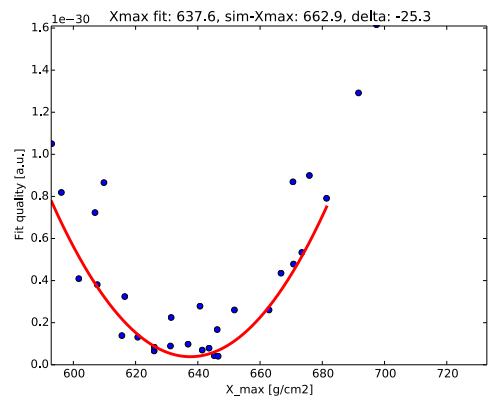


**Figure 4.** Fit quality as a function of  $X_{\max}$ .

### 3 Results

The offset in  $X_{\max}$  per 10% change in refractivity has been evaluated for four zenith angles in the range of 15 to 45 degrees. For each shower in the ensemble, the difference between fitted and simulated  $X_{\max}$  is shown in Fig. (5). A quadratic fit to the points is shown.

A modeled offset is calculated from the simplistic assumption that the radio footprint would scale (only) with the size of the Cherenkov cone, starting at the  $X_{\max}$  altitude. The offsets thus found

are nearly twice as large as those found from full simulations. This indicates that Cherenkov time compression is not the only factor that sets the shape of the radio footprint, as is known for lower frequencies ( $< 100$  MHz).

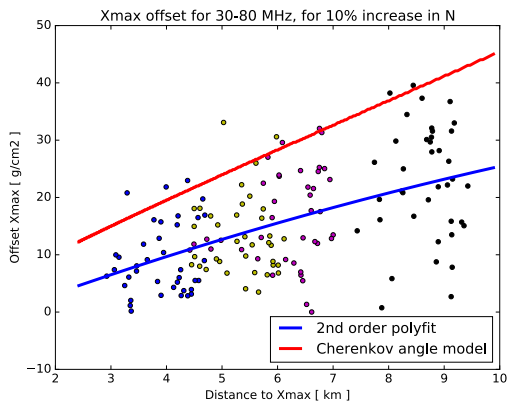


**Figure 5.** Results for the LOFAR low-band frequency range, 30 – 80 MHz.

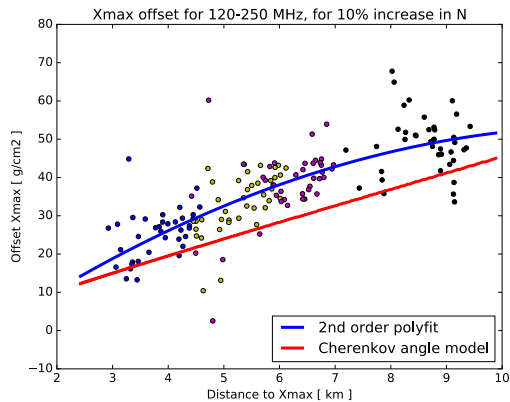


**Figure 6.** Results for a higher-frequency range, 120 – 250 MHz.

## 4 Summary

For mass composition analysis, the accuracy of  $X_{\max}$  measurements is critical. Here, we have simulated the systematic error due to variations in the atmospheric refractive index. For the 30 – 80 MHz band, a 10% change in refractivity yields changes in inferred  $X_{\max}$  from 8 to 22 g/cm<sup>2</sup> for zenith angles ranging from 15 to 45 degrees. At higher frequencies, 120–250 MHz, the range is 20 to 45 g/cm<sup>2</sup>, and agrees qualitatively with a toy model based on the Cherenkov angle at the  $X_{\max}$  altitude.

Realistic corrections to the CoREAS default refractivity are on the order of 4%, leading to a zenith-angle dependent bias of up to about 10 g/cm<sup>2</sup>. Including local atmospheric data per air shower into the simulations is a subject of further investigation.

## References

- [1] A. Aab et al. (Pierre Auger Collaboration), *Phys. Rev. D* **93**, 122005 (2016)
- [2] S. Buitink et al., *Phys. Rev. D* **90**, 082003 (2014)
- [3] M.P. van Haarlem et al., *A & A* **556**, A2 (2013), 1305 . 3550
- [4] K.H. Kampert, M. Unger, *Astroparticle Physics* **35**, 660 (2012)
- [5] S. Buitink et al., *Nature p.* 70 (2016)
- [6] P. Schellart, A. Nelles, et al. LOFAR collaboration, *A & A* **560**, A98 (2013), 1311 . 1399
- [7] T. Huege, M. Ludwig, C.W. James, *AIP Conference Proceedings* **1535**, 128 (2013)
- [8] D. Heck et al., *CORSIKA: a Monte Carlo code to simulate extensive air showers.* (1998)
- [9] U.S. Government Printing Office (1976)
- [10] J. Rieger, *Proceedings of FIG XXII International Congress, 2002* (2002)
- [11] National Oceanic and Atmospheric Administration, *Global Data Assimilation System* (2016)
- [12] A. Nelles, P. Schellart et al., *Astroparticle Physics* **65**, 11 (2015)